

Soft Core Plane State Structures Under Static Loads Using GDQFEM and Cell Method

E. Viola¹, F. Tornabene¹, E. Ferretti¹ and N. Fantuzzi¹

Abstract: The aim of this work is to study the static behavior of 2D soft core plane state structures. Deflections and inter-laminar stresses caused by forces can have serious consequences for strength and safety of these structures. Therefore, an accurate identification of the variables in hand is of considerable importance for their technical design. It is well-known that for complex plane structures there is no analytical solution, only numerical procedures can be used to solve them. In this study two numerical techniques will be taken mainly into account: the Generalized Differential Quadrature Finite Element Method (GDQFEM) and the Cell Method (CM). The former numerical technique is based on the classic Generalized Differential Quadrature (GDQ) rule and operates differently from the classic Finite Element Method (FEM). The principal novelty of this paper regards the comparison, by means of several numerical applications about soft-core structures, among GDQFEM, CM and FEM. Such a comparison appears for the first time in the literature and in this paper.

Keywords: Generalized Differential Quadrature Finite Element Method, Soft-Core Structures, Sandwich Structures, Cell Method.

1 Introduction

The Finite Element Method (FEM) has always been considered a robust and strong tool for solving many engineering problems, such as the ones concerning composite laminated structures. Over the years, many scientists have tried new ways for analysing these types of structures using faster and more accurate numerical procedures [Li, Shen, Han, and Atluri (2003); Sladek, Sladek, and Atluri (2004); Han, Liu, Rajendran, and Atluri (2006); Li and Atluri (2008b,a)]. The main FEM idea is that a generic domain can be divided into several small parts (called elements) where the solution is found using a certain field approximation. In this paper a

¹ DICAM Department, University of Bologna, Italy.

Generalized Differential Quadrature Finite Element Method (GDQFEM) is presented. This numerical technique is based on the Generalized Differential Quadrature (GDQ) method which can solve a differential system of equations on a regular domain. The most important contributions about GDQ were brought by Shu [Shu (2000)], nevertheless this technique has expanded over the years. The first seminal references about the application of GDQ to civil structures are given by the works [Artioli, Gould, and Viola (2005); Viola, Dilena, and Tornabene (2007); Marzani, Tornabene, and Viola (2008)]. Subsequently, the authors deepen their knowledge about GDQ discretization types and convergence rate of the technique on shells of revolution in the papers [Tornabene and Viola (2009a,b, 2013); Viola, Rossetti, and Fantuzzi (2012)]. Only recently higher-order theories have been studied for the static and dynamic analysis of composite multi-layered shells and plates [Tornabene and Ceruti (2013a,b); Tornabene and Reddy (2014); Tornabene, Fantuzzi, Viola, and Carrera (2014)]. GDQFEM works in the same way as FEM, by subdividing the whole domain into several sub-domains of regular and irregular shapes. The only difference between FEM and GDQFEM is that the system of equations is solved in the weak or in the strong form, respectively. In fact, both methods have a discretization procedure and the irregular elements are processed by a mapping technique. The system of equations is actually solved on a parent domain instead of the physical one. A good introduction to the GDQFEM can be found in [Fantuzzi (2013)], where the treatment of the boundary conditions is also reported, which is a key point of the numerical technique. In addition, in order to understand the problem of boundary conditions implementation in GDQFEM, the interested reader can refer to [Chen (1999a,b, 2000, 2003)]. It should be noted that, when the strong form of the formulated system of equations is solved, the accuracy of the solution to the problem under consideration is higher than the same solution calculated starting from a standard weak formulation. It has been proven in [Tornabene, Viola, and Fantuzzi (2013); Viola, Tornabene, and Fantuzzi (2013a,c)] that using 2D theories and GDQ method it is possible to have very accurate solutions compared to 3D FEM. In the present paper, the numerical results obtained with this numerical technique will be compared to the ones calculated according to the well-known FEM, the Cell Method (CM) and other results found in literature. As far as the CM method is concerned, it was initially developed by Tonti [Tonti (2001)]. In the subsequent years Ferretti made several applications in the works [Ferretti (2001, 2003, 2004a,b,c, 2005); Ferretti, Casadio, and Leo (2008); Ferretti (2009, 2012)]. Recently new applications of CM appeared in literature [Ferretti (2014, 2013a,b)]. Summarizing, this paper is mainly divided into three parts. After a brief introduction to the problem in the present section, the theoretical development of GDQFEM is shown in the third section. Finally, some numerical applications are reported in the fourth section. In particular, the free vibrations of a sandwich beam are anal-

used in two parts. In the beginning the GDQFEM solution is compared with some literature results where the mechanical properties of the core are fixed. Then, considering the same structure and varying the core stiffness, the natural frequencies are shown in order to see the code accuracy in the presence of a highly-soft-core structure. In the second example another cantilever sandwich beam is worked out under static loading. In this case the numerical GDQFEM solution is compared to a CM and FEM solutions. Very good agreement among the results of all the used methodologies is verified. In conclusion, in order to see the GDQFEM stability when curved plane structures are investigated, a sandwich circular arch is numerically solved under static loading and its mode shapes are calculated. To the best of the authors' knowledge, the comparison in hand has never appeared in literature.

2 2D elastic problem

This section is devoted to a concise presentation of the well-known general formulation of boundary value problems in plane elasticity. The equilibrium equations for a 2D elastic body can be derived from 3D elasticity

$$\begin{aligned}\frac{\partial \sigma_x}{\partial x} + \frac{\partial \tau_{xy}}{\partial y} + f_x &= 0 \\ \frac{\partial \tau_{xy}}{\partial x} + \frac{\partial \sigma_y}{\partial y} + f_y &= 0\end{aligned}\quad (1)$$

In Eq. 1 σ_x , σ_y , τ_{xy} are the normal and shear stresses and f_x , f_y denote the body forces. When a plain strain case is considered, the constitutive equations can be written as

$$\sigma_x = 2G\varepsilon_x + \lambda I_{1\varepsilon}, \quad \sigma_y = 2G\varepsilon_y + \lambda I_{1\varepsilon}, \quad \sigma_z = \lambda I_{1\varepsilon}, \quad \tau_{xy} = G\gamma_{xy}\quad (2)$$

where $I_{1\varepsilon} = \varepsilon_x + \varepsilon_y$ is the cubic dilation and G , λ are the shear modulus and the second Lamé constant, respectively. The kinematic relationships are

$$\varepsilon_x = \frac{\partial u}{\partial x}, \quad \varepsilon_y = \frac{\partial v}{\partial y}, \quad \gamma_{xy} = \frac{\partial u}{\partial y} + \frac{\partial v}{\partial x}\quad (3)$$

where $u = u(x, y)$, $v = v(x, y)$ are the displacement components defined on the plane domain of the structure. In conclusion, using Eq. 3, Eq. 2, Eq. 1 and adding the inertia forces, the fundamental system of equations in its strong form can be found

$$\begin{aligned}(\lambda + 2G) \frac{\partial^2 u}{\partial x^2} + G \frac{\partial^2 u}{\partial y^2} + (\lambda + G) \frac{\partial^2 v}{\partial x \partial y} + f_x &= \rho \frac{\partial^2 u}{\partial t^2} \\ (\lambda + 2G) \frac{\partial^2 v}{\partial y^2} + G \frac{\partial^2 v}{\partial x^2} + (\lambda + G) \frac{\partial^2 u}{\partial x \partial y} + f_y &= \rho \frac{\partial^2 v}{\partial t^2}\end{aligned}\quad (4)$$

In order to solve the differential system of static and dynamic equations at hand, the boundary conditions have to be enforced. In general boundary conditions can be kinematic and static kind. The first type, called kinematic boundary condition, is enforced on the displacements u and v , and the second type, called static boundary condition, is imposed on the stresses σ_n and τ_{ns} which follow the outward unit normal vector \mathbf{n} at a generic point of the boundary. According to the work by [Viola, Tornabene, and Fantuzzi (2013b)] the normal and shear stresses of a local reference system $n_s z$ can be written as a function of the Cartesian system xyz as

$$\begin{aligned} \sigma_n &= \sigma_x n_x^2 + \sigma_y n_y^2 + 2\tau_{xy} n_x n_y \\ \tau_{ns} &= (\sigma_y - \sigma_x) n_x n_y + \tau_{xy} (n_x^2 - n_y^2) \end{aligned} \tag{5}$$

It is noted that n_x, n_y are the direction cosines of the edge of normal \mathbf{n} . In other words n_x, n_y are the components of the unit vector \mathbf{n} .

3 Generalized differential quadrature finite element method

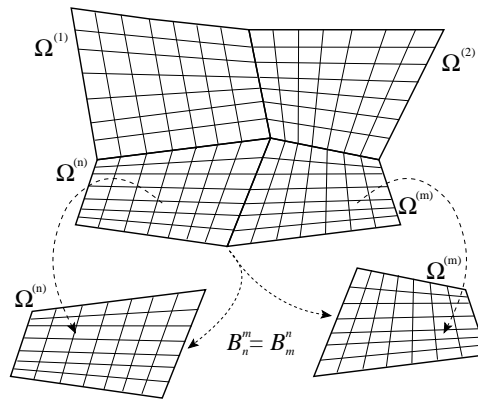


Figure 1: Multi-domain decomposition with interface boundaries and external boundaries.

GDQFEM is an advanced version of the multi-domain technique, which subdivides a physical domain into several regular sub-domains (such as rectangles and squares). However, when curved boundaries and distorted elements are necessary to approximate the physical problem a mapping technique must be used. Taking Fig. 1 as a sample mesh composed of four distorted elements, the generic element $\Omega^{(n)}$ must be mapped into a regular domain (parent element) in order to apply the GDQ method at the master element level. The similarity with FEM is obvious, nevertheless a big difference occurs between the two approaches. In fact, GDQFEM

is based on the strong form of the differential system of equations, on the contrary FEM solves the weak form of the same differential problem. The GDQFEM requires each sub-domain to be regular like any other low-order finite difference scheme. Thus, GDQ cannot be applied directly as in regular multi-domain differential quadrature. The Cartesian coordinate transformation is indicated as

$$x = x(\xi, \eta), \quad y = y(\xi, \eta) \quad (6)$$

where Eq. 6 gives a two-way mapping from the physical space (x, y) to the parent element space (ξ, η) , and vice versa. For the sake of conciseness, the mathematical developments of the mapping technique are not reported in the following, but the interested reader can find all the relationships in detail in a number of works [Bert and Malik (1996); Shu, Chen, and Du (2000); Xing and Liu (2009); Xing, Liu, and Liu (2010)]. Once the physical element is mapped into the computational domain, GDQ can be applied. The generalized differential quadrature (GDQ) method is a very powerful numerical technique that permits to evaluate partial and total derivatives through a sum of functional values multiplied by certain weights. The interested reader can find a brief review on GDQ applications in [Tornabene (2009, 2012); Viola and Tornabene (2005, 2006, 2009)]. Following the idea of integral quadrature, the first order derivative of one-variable functions, e.g. $f(x)$, can be written as

$$\left. \frac{df(x)}{dx} \right|_{x=x_i} = f_x^{(1)}(x_i) = \sum_{j=1}^N a_{ij}^{x,(1)} f(x_j) \quad \text{for } i = 1, 2, \dots, N \quad (7)$$

where $a_{ij}^{x,(1)}$ represent the weighting coefficients, N is the total number of grid points x_1, x_2, \dots, x_N in the whole domain and $f(x_j)$ is the calculated value of $f(x)$ at the point $x = x_j$. From Eq. 7 it appears that, when the weighting coefficients are computed, the derivative of the $f(x)$ function at the point $x = x_i$ is given by the sum of values calculated according to the right-hand of Eq. 7. Thus, it is compulsory to have a well-defined grid point distribution all over the given domain. Several GDQ grid distributions samples are reported in [Tornabene and Viola (2008); Tornabene (2011a,b,c)]. To compute the first order weighting coefficients $a_{ij}^{x,(1)}$, the following algebraic formulae are derived

$$a_{ij}^{x,(1)} = \frac{L^{(1)}(x_i)}{(x_i - x_j)L^{(1)}(x_j)} \quad \text{for } i, j = 1, 2, \dots, N \text{ and } i \neq j$$

$$a_{ii}^{x,(1)} = - \sum_{k=1, k \neq i}^N a_{ik}^{(1)} \quad \text{for } i = j \quad (8)$$

where the Lagrange interpolation polynomials L were used as test functions

$$L^{(1)}(x_i) = \prod_{q=1, q \neq i}^N (x_q - x_i), \quad L^{(1)}(x_j) = \prod_{q=1, q \neq j}^N (x_q - x_j) \tag{9}$$

The weighting coefficients of the second and higher order derivatives can be computed from recurrence relationships. A generalized higher order derivative can be written as

$$\left. \frac{d^n f(x)}{dx^n} \right|_{x=x_i} = f_x^{(n)}(x_i) = \sum_{j=1}^N a_{ij}^{x,(n)} f(x_j) \tag{10}$$

for $i = 1, 2, \dots, N, n = 2, 3, \dots, N - 1$

This general approach, as shown in [Tornabene and Viola (2007)], which is based on the polynomial approximation, allows to write the following weighting coefficients

$$a_{ij}^{x,(n)} = n \left(a_{ii}^{x,(n-1)} a_{ij}^{x,(1)} - \frac{a_{ij}^{x,(n-1)}}{x_i - x_j} \right) \quad \text{for } i \neq j, n = 2, 3, \dots, N - 1 \tag{11}$$

$$a_{ii}^{x,(n)} = - \sum_{k=1, k \neq i}^N a_{ik}^{x,(n)} \quad \text{for } i = j$$

As shown in the works [Tornabene, Marzani, Viola, and Elishakoff (2010); Tornabene, Viola, and Inman (2009)], the one-dimensional problem can be directly extended to the multi-dimensional case for a regular shape, such as a rectangle or a circle. In general, a function $f(x, y)$ can be defined on the given domain and its values depend on the points along x and y . In the following, N points along x direction and M points along y direction are assumed. It is noted that the derivatives of any order along x and y can be written as

$$f_x^{(n)}(x_i, y_j) = \left. \frac{\partial^{(n)} f(x, y)}{\partial x^n} \right|_{\substack{x=x_i \\ y=y_j}} = \sum_{k=1}^N a_{ik}^{x,(n)} f(x_k, y_j) \tag{12}$$

for $i = 1, 2, \dots, N \quad n = 1, 2, \dots, N - 1$

$$f_y^{(m)}(x_i, y_j) = \left. \frac{\partial^{(m)} f(x, y)}{\partial y^m} \right|_{\substack{x=x_i \\ y=y_j}} = \sum_{l=1}^M a_{jl}^{y,(m)} f(x_i, y_l)$$

for $j = 1, 2, \dots, M \quad m = 1, 2, \dots, M - 1$

where $a_{ik}^{x,(n)}$ and $a_{jl}^{y,(m)}$ are the weighting coefficients of order n and m along x and y , respectively. Moreover, following the same rule of Eq. 12, the mixed derivative

can be written as follows

$$f_{xy}^{(n+m)}(x_i, y_j) = \frac{\partial^{(n+m)} f(x, y)}{\partial x^n \partial y^m} \Bigg|_{\substack{x=x_i \\ y=y_j}} = \sum_{k=1}^N a_{ik}^{x,(n)} \left(\sum_{l=1}^M a_{jl}^{y,(m)} f(x_k, y_l) \right) \quad (13)$$

for $i = 1, 2, \dots, N$ $j = 1, 2, \dots, M$
for $n = 1, 2, \dots, N-1$ $m = 1, 2, \dots, M-1$

where $a_{ik}^{x,(n)}$ and $a_{jl}^{y,(m)}$ have the same meaning of the ones in Eq. 12.

The aforementioned GDQ procedure is used at the master element level. Consider a general physical domain that has to be decomposed into elements in order to capture the domain discontinuities of material and geometry. In particular, the physical domain Ω is divided into several $\Omega^{(n)}$ elements, where $n = 1, 2, \dots, n_e$. It is worth noticing that $\Omega^{(n)} \cap \Omega^{(m)} = \emptyset$ and $\Omega = \Omega^{(1)} \cup \Omega^{(2)} \cup \dots \cup \Omega^{(n_e)}$. As a result, there is no relation between the element $\Omega^{(n)}$ and $\Omega^{(m)}$, they are only connected among their edges.

A GDQFEM element is made of three groups of points: the domain points, the boundary points and the corner points. The first set is used for the discretized form of the fundamental system of equations. In the second set, the external boundary conditions and the inter-element compatibility conditions have to be imposed. The last group is necessary for the boundary conditions too, but the corner points must be treated differently due to their belonging to two adjacent edges. For further details on how the corner type boundary conditions are considered, the reader should follow the works [Karami and Malekzadeh (2003); Liu (1999); Zhong and He (1998); Zhong and Yu (2009)], among others.

Since GDQ is a global collocation method, the stiffness matrix of each element contains the boundary and domain equations in algebraic form. The assembly procedure follows the well-known rules of FEM, through the connectivity matrix of the mesh. Thus, once the assembly procedure is completed, the explicit algebraic form of a GDQFEM differential system is very similar to a classic GDQ solution [Tornabene, Fantuzzi, Viola, and Reddy (2013); Tornabene, Fantuzzi, Viola, and Ferreira (2013); Ferreira, Viola, Tornabene, Fantuzzi, and Zenkour (2013)]. Hence, the final static case can be reported in matrix compact form as

$$\begin{bmatrix} \bar{\mathbf{K}}_{bb} & \bar{\mathbf{K}}_{bd} \\ \bar{\mathbf{K}}_{db} & \bar{\mathbf{K}}_{dd} \end{bmatrix} \begin{bmatrix} \mathbf{U}_b \\ \mathbf{U}_d \end{bmatrix} = \begin{bmatrix} \mathbf{Q}_b \\ \mathbf{Q}_d \end{bmatrix} \quad (14)$$

where \mathbf{U}_b and \mathbf{U}_d indicate the bounded and domain displacement parameters vectors, \mathbf{Q}_b and \mathbf{Q}_d represent the vector of the external forces applied at the boundary and domain points. In other words, they are the boundary and domain loads. Finally the global stiffness matrix is shown divided into four sub-matrices: $\bar{\mathbf{K}}_{bb}$ and

$\bar{\mathbf{K}}_{bd}$ are the matrices of the external boundary and compatibility conditions and $\bar{\mathbf{K}}_{db}$ and $\bar{\mathbf{K}}_{dd}$ are the matrices of the fundamental equations (domain equations). For the sake of clarity, a sample of a GDQFEM global stiffness matrix is represented in Fig. 2a), for a mesh composed of two elements. In particular the boundary points are located in the upper part, whereas the domain points are positioned in the lower part. It is noted that the domain matrices $\mathbf{K}_{dd}^{(1)}$, $\mathbf{K}_{dd}^{(2)}$ and $\mathbf{K}_{db}^{(1)}$, $\mathbf{K}_{db}^{(2)}$ are diagonally dominant. On the contrary the boundary matrices $\mathbf{K}_{bb}^{(1)}$, $\mathbf{K}_{bb}^{(2)}$ and $\mathbf{K}_{bd}^{(1)}$, $\mathbf{K}_{bd}^{(2)}$ and $\mathbf{K}_{bb}^{(1,2)}$, $\mathbf{K}_{bb}^{(2,1)}$ and $\mathbf{K}_{bd}^{(1,2)}$, $\mathbf{K}_{bd}^{(2,1)}$ form a full matrix. In fact aside from the boundary matrices for every single element $\mathbf{K}_{bb}^{(n)}$, $\mathbf{K}_{bd}^{(n)}$ (for $n = 1, 2$) there are the matrices of the compatibility conditions $\mathbf{K}_{bb}^{(n,m)}$, $\mathbf{K}_{bd}^{(n,m)}$ (for $n, m = 1, 2$).

When the free vibration problem is considered, a generalized eigenvalue problem have to be solved

$$\begin{bmatrix} \bar{\mathbf{K}}_{bb} & \bar{\mathbf{K}}_{bd} \\ \bar{\mathbf{K}}_{db} & \bar{\mathbf{K}}_{dd} \end{bmatrix} \begin{bmatrix} \mathbf{U}_b \\ \mathbf{U}_d \end{bmatrix} = \omega^2 \begin{bmatrix} \mathbf{0} & \mathbf{0} \\ \mathbf{0} & \bar{\mathbf{M}}_{dd} \end{bmatrix} \begin{bmatrix} \mathbf{U}_b \\ \mathbf{U}_d \end{bmatrix} \tag{15}$$

The stiffness matrix remains the same as the static case; the mass matrix is diagonally dominant. A mass matrix sample, for a two element mesh, is shown in Fig. 2b). There is not a mass definition on the boundary points, because in the present study any concentrated mass has been considered in any computation. Only distributed masses due to material density are imposed.

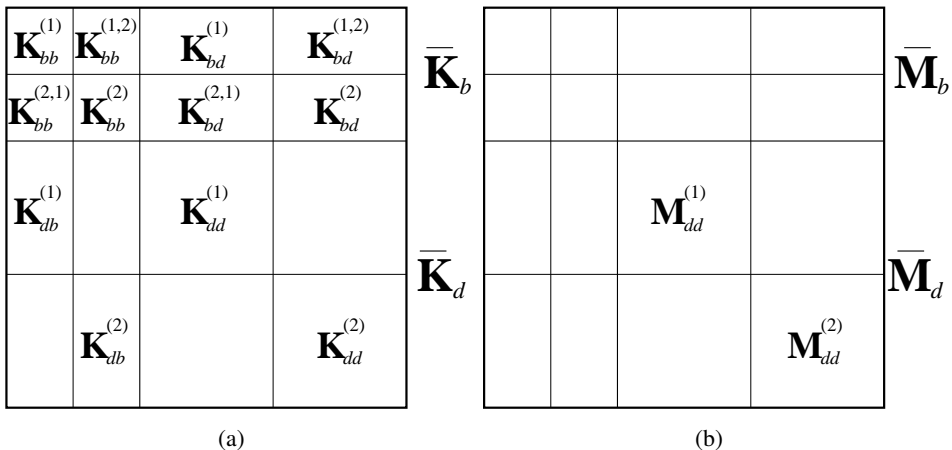


Figure 2: Global GDQFEM matrices for a two element mesh: a) Stiffness matrix; b) Mass matrix.

In general, when a GDQ algebraic system has to be solved, a grid distribution

Table 1: First ten natural frequencies for a cantilever elastic beam.

f [Hz]	FEM [†]	MLPG [†]	NBNM [†]	EFG [†]	$n_e = 1$ $N = 41$	$n_e = 3$ $N = 21$
1	821.059	824.44	844.19	811.63	822.08	822.08
2	4925.76	5070.32	5051.21	4907.9	4931.61	4931.60
3	12823.2	12894.73	12827.6	12852	12823.20	12823.20
4	12975.4	13188.12	13258.2	13075	12989.85	12989.84
5	23581.1	24044.43	23992.8	24113	23605.51	23605.48
6	35964.9	36596.15	36432.2	37463	36000.21	36000.16
7	38440.5	38723.9	38436.4	38616	38441.64	38441.63
8	49516.7	50389.01	49937.2	51999	49564.38	49564.31
9	63831.7	64413.89	63901.2	64566	63894.24	63894.16
10	63965.6	64937.83	64085.9	68585	63970.67	63970.64

[†] [Amirani, Khalili, and Nemati (2009)]

must be chosen [Tornabene, Liverani, and Caligiana (2011, 2012a,b,c)]. In the present case, a Chebyshev-Gauss-Lobatto (C-G-L) grid has been considered in all the computations

$$\begin{aligned}\xi_i &= -\cos\left(\frac{i-1}{N-1}\pi\right), \text{ for } i = 1, \dots, N \\ \eta_j &= -\cos\left(\frac{j-1}{N-1}\pi\right), \text{ for } j = 1, \dots, M\end{aligned}\tag{16}$$

It has been demonstrated in literature by [Tornabene (2009); Tornabene, Fantuzzi, Viola, Cinefra, Carrera, Ferreira, and Zenkour (2014)] that this grid leads to very accurate results. The number of grid points along the two element sides are indicated by N , M . In order to always have compatibility between all the GDQFEM elements an equal number of grid points will be considered, therefore N will stand for $N = M$.

4 Numerical applications

Homogeneous elastic cantilever beam

As a first numerical benchmark a homogeneous and isotropic elastic cantilever beam is considered in the following. The mechanical properties of the beam are $E = 205.939$ GPa, $\nu = 0.3$, $\rho = 7845.32$ kg/m³.

Table 2: First ten frequencies for a fully clamped sandwich cantilever beam.

f [Hz]	FEM [†]	EFG [†]	$n_e = 3$ $N = 21$	$n_e = 3$ $N = 31$
1	21.5438	21.93	21.5620	21.5632
2	93.998	97.07	94.2283	94.2307
3	200.354	207.9	201.0721	201.0765
4	307.277	319.12	308.8174	308.8408
5	417.978	432.88	420.8502	420.8787
6	531.631	547.97	536.3943	536.4781
7	651.009	667.01	658.3320	658.4971
8	776.451	790.25	786.1107	787.3466
9	909.587	919.32	928.6953	924.6957
10	1050.72	1054.06	1136.3864	1070.8950

[†] [Amirani, Khalili, and Nemati (2009)]

The beam length is $L = 0.10$ m and height equal to $D = 0.01$ m. The thickness of the investigated structures, except where otherwise stated, is equal to 0.001 m. In Tab. 1, the GDQFEM solutions are obtained with a single element mesh $n_e = 1$ with $N = 41$ and a three-element mesh $n_e = 3$ with $N = 21$. The numerical results carried out with the current methodology are compared with the results reported by [Amirani, Khalili, and Nemati (2009)]. Very good agreement among all the theories is observed and the interested reader should refer to the paper just above mentioned to gain the knowledge of the numerical methods (MLPG, NBNM, EFG) reported in Tab. 1.

4.1 Sandwich cantilever beam

In the second example, a sandwich cantilever beam composed of two sheets and a soft-core is considered (see Fig. 3). The beam length is $L = 1$ m and the height $D = 0.02$ m. The core thickness is $t_c = 1.4 \cdot 10^{-2}$ m and the two face sheets are $t_f = 3 \cdot 10^{-3}$ m. Both the two constituent materials are isotropic. The soft-core has an elastic modulus $E_c = 0.2$ GPa, a Poisson's ratio $\nu_c = 0.27$ and a density $\rho_c = 60$ kg/m³, whereas the two sheets have $E_f = 200$ GPa, $\nu_f = 0.3$ and $\rho_f = 7800$ kg/m³. The validation of the present code considers a fully and a partially clamped beam. The fully clamped beam is depicted in Fig. 3, where the partially clamped has the top and bottom plies clamped and the soft core free. These two models were compared with FEM and EFG by [Amirani, Khalili, and Nemati (2009)].

In Tab. 2 and Tab. 3, the first ten frequencies of a fully clamped and partially

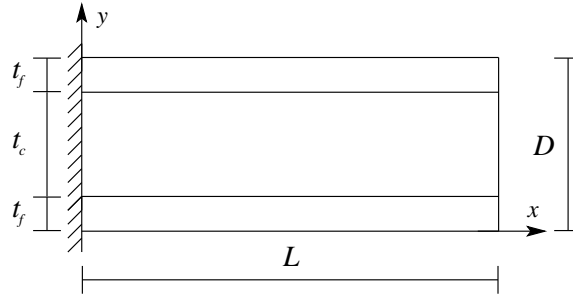


Figure 3: A sandwich beam geometric model.

Table 3: First ten frequencies for a partially clamped sandwich cantilever beam.

f [Hz]	FEM‡	EFG†	$n_e = 3$ $N = 21$	$n_e = 3$ $N = 31$
1	21.5437	21.92	21.5643	21.5575
2	93.9951	96.81	94.2207	94.2002
3	200.346	207.24	201.0034	200.8917
4	307.264	318.1	308.7793	308.2736
5	417.961	431.49	420.6148	420.6976
6	531.609	546.14	536.3559	536.3396
7	650.981	664.67	658.6543	658.4117
8	776.418	787.28	779.5960	787.0041
9	909.547	915.61	904.8425	925.1526
10	1050.67	1049.9	1131.9594	1070.3390

† [Amirani, Khalili, and Nemati (2009)]

‡ 2D ABAQUS CPS8R plane elements

clamped cantilever beam are reported, respectively. In particular, the GDQFEM results obtained with a three elements mesh $n_e = 3$ and two sets of grid points $N = 21$ and $N = 31$ are compared with a FEM solution and a reference EFG solution. It should be noted that, when a three-element mesh is used, a single GDQFEM element refer to each layer layer. In addition, from Tabs. 2-3 it appears that GDQFEM solutions are in very good agreement with the two reference solutions. The results of the partially clamped case are lower than those obtained with the fully clamped case, due to the effect of less constrained boundary conditions.

To study the effect of core flexibility on the natural frequencies of the sandwich beam, a parametric analysis is performed. All the numerical results are compared

Table 4: First ten natural frequencies of sandwich beams with various cores

χ	0.0001		0.001		0.01		0.1	
f [Hz]	EFG [†]	$n_e = 3$ $N = 31$	EFG [†]	$n_e = 3$ $N = 31$	EFG [†]	$n_e = 3$ $N = 31$	EFG [†]	$n_e = 3$ $N = 31$
1	13.744	13.40	21.93	21.56	24.085	23.77	25.08	24.58
2	45.235	44.70	97.07	94.23	141.64	139.30	155.82	152.70
3	85.857	86.77	207.9	201.08	364.23	356.48	430.59	421.75
4	129.63	135.08	319.12	308.84	645.17	628.03	828.52	810.72
5	181.01	194.44	432.88	420.88	960.92	930.75	1339.4	1308.72
6	240.41	265.12	547.97	536.48	1275.5	1249.23	1421	1393.58
7	309.26	348.60	667.01	658.50	1294.9	1269.31	1950	1901.87
8	388.13	444.90	790.25	787.35	1638.1	1575.31	2647.2	2576.28
9	477.52	554.53	919.32	924.70	1985.3	1904.92	3418.3	3318.73
10	577.98	677.41	1054.06	1070.90	2334.6	2236.38	4251.9	4117.36

[†] [Amirani, Khalili, and Nemati (2009)]

with the ones obtained by [Amirani, Khalili, and Nemati (2009)] and they are reported in Tab. 4. The stiffness factor $\chi = E_c/E_f$ is defined as the ratio of the elastic moduli of the core to the two sheets. For $\chi = 1$, a homogeneous elastic system is derived. When χ decreases the core tends to be softer than the two sheets. On the contrary when χ increases the opposite behavior occurs. From Tab. 4, it is noted that when the stiffness factor decreases it leads to lower natural frequencies of the structure.

4.2 Static analysis of a cantilever sandwich beam

In the following third example, the static analysis of a cantilever sandwich beam is considered. The investigated example is reported in the book by [Zong and Zhang (2009)], where the mechanical properties of the core and the two sheets are $E_c = 1.67$ GPa, $E_f = 0.167$ GPa, $\nu_c = \nu_f = 0.3$. Considering Fig. 3 as a reference, the geometric characteristics of the beam are length $L = 4.8$ m and height $D = 1.2$ m. In particular, the thickness of the core is $t_c = 0.8$ m and $t_f = 0.2$ m, for each of the two sheets. A static uniform vertical load is applied at the top layer and indicated by $q = 100$ Pa. In the following, several through-the-thickness quantities such as displacements and stresses are compared to FEM and CM solutions. All of the plots, graphically presented in Figs. 4-7 show three curves: the solid blue curve indicates the CM solution; the curve made of black crosses denotes the FEM solution and the line composed of black circles stands for the GDQFEM solution. Such GDQFEM solution is obtained with three elements only $n_e = 3$ and $N = 21$

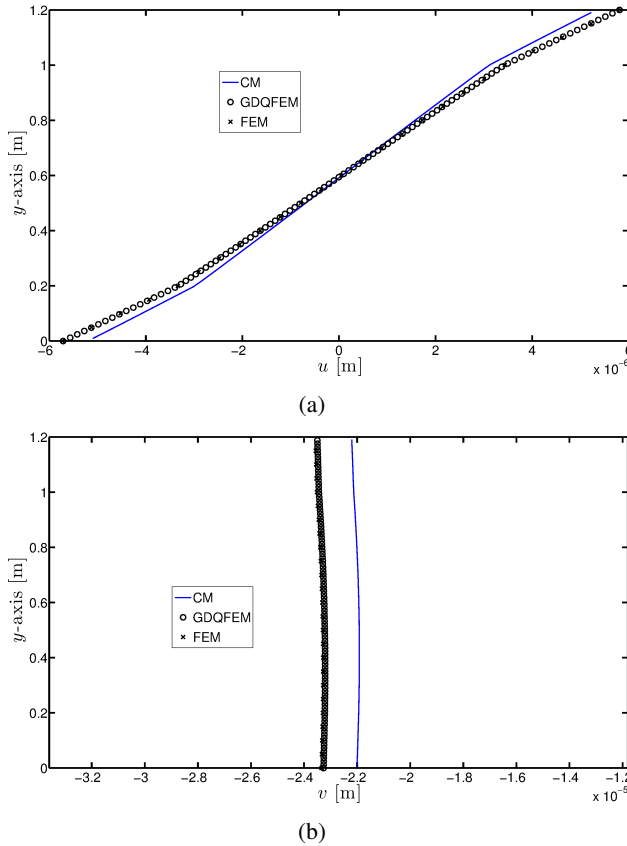
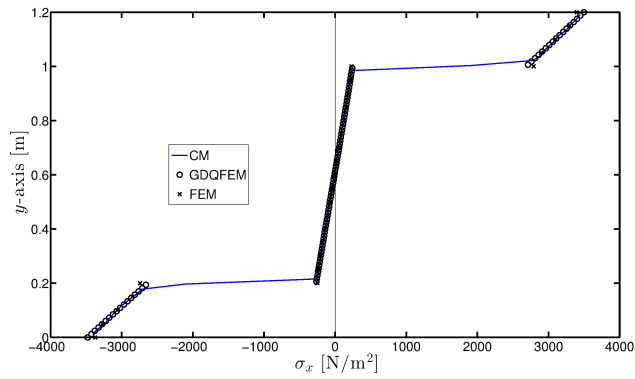


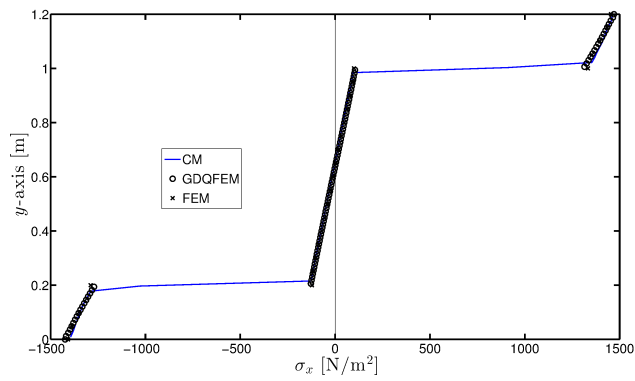
Figure 4: Displacements at the middle section $x = 2.4$ m: a) horizontal displacement u ; b) vertical displacement v .

grid points. Three different sections are studied in this example. They are located at $x = 1.2$ m, $x = 2.4$ m and $x = 3.6$ m.

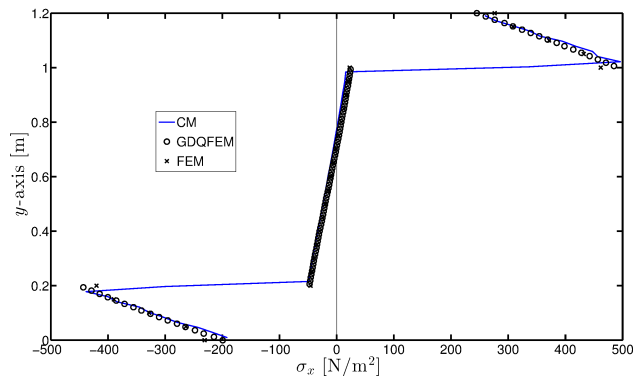
In Fig. 4, the horizontal and vertical displacements are shown at $x = 2.4$ m. It can be noticed that the GDQFEM and FEM solutions are superimposed and there is a slight difference with the CM numerical solution. As far as the stress components are concerned, Figs. 5-7 show the stress recovery solution for the problem under consideration. In particular, the normal stress σ_x is computed at three distinct sections for the three numerical methods illustrated above. It is noted that, in Figs. 5a),b) the stress profiles have the same shape, whereas the tendency of the curves on the two sheets changes in Fig. 5c). In fact, in Fig. 5c) the maximum normal stress σ_x is calculated at the two material interfaces, whereas in Figs. 5a),b) the



(a)

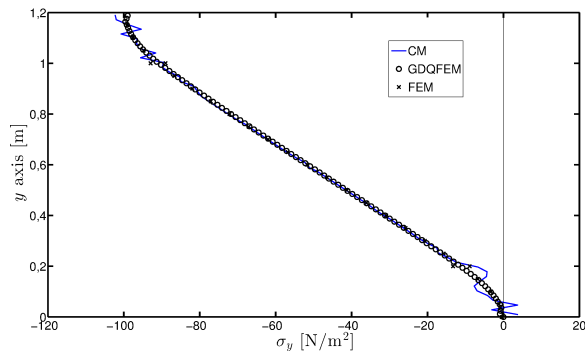


(b)

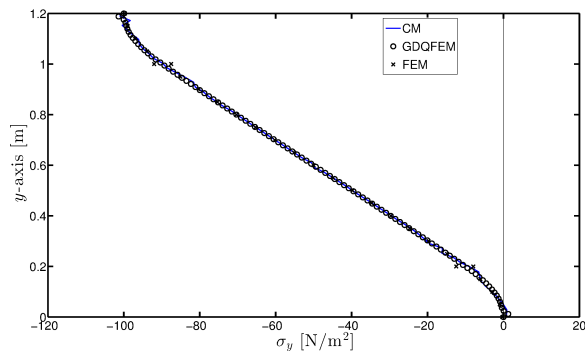


(c)

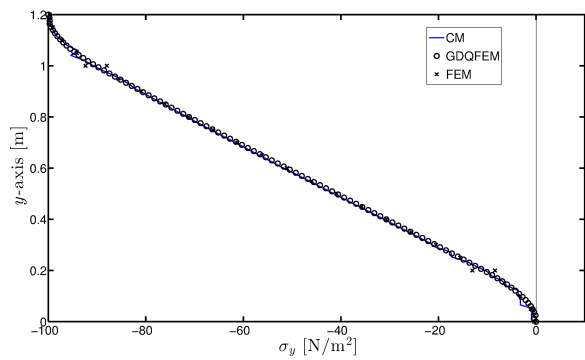
Figure 5: Normal stress σ_x evaluated at: a) $x = 1.2$ m, b) $x = 2.4$ m and c) $x = 3.6$ m.



(a)

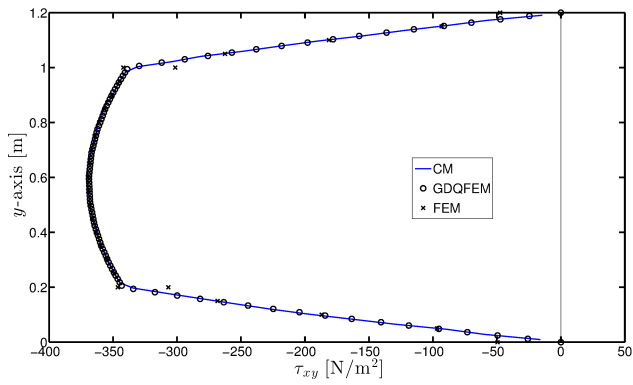


(b)

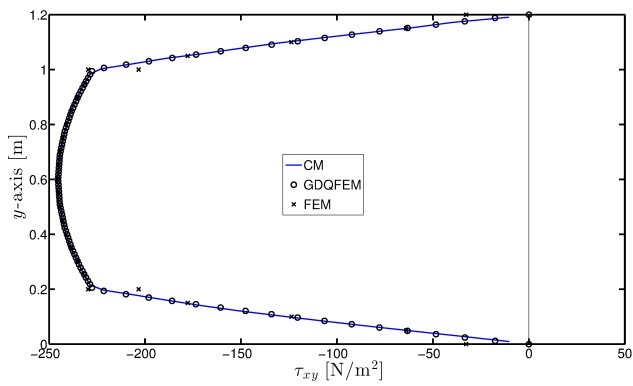


(c)

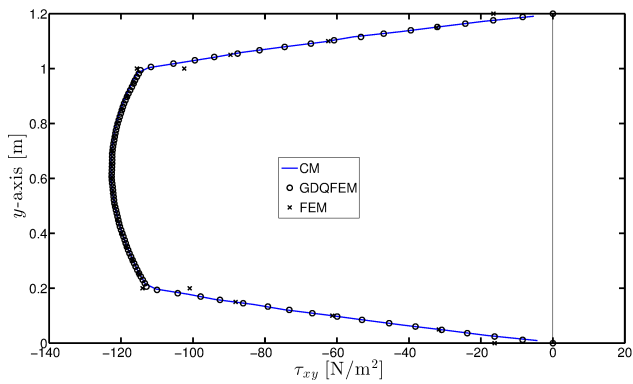
Figure 6: Normal stress σ_y evaluated at: a) $x = 1.2$ m, b) $x = 2.4$ m and c) $x = 3.6$ m.



(a)



(b)



(c)

Figure 7: Shear stress τ_{xy} evaluated at: a) $x = 1.2$ m, b) $x = 2.4$ m and c) $x = 3.6$ m.

maximum stress is at the top and bottom of the sandwich. All the three numerical results are superimposed in all the representations.

Regarding the transversal stress σ_y at the three beam sections at issue, the corresponding through-the-thickness profiles are depicted in Figs. 6a)-c). In particular, each σ_y curve is continuous through the beam thickness. The CM, GDQFEM, FEM numerical solutions are generally in good agreement. The CM solution shows an oscillating character at $x = 1.2$ m. On the other hand, the FEM solution shows more values at each interface. This happens because the FEM solver has to deal with material properties which are different between two adjacent elements. It should be noted that the σ_y stress profiles satisfy the boundary conditions at the top and bottom sections of the investigated cantilever sandwich beam. The last comparison involving the shear stress τ_{xy} is represented in Figs. 7a)-c). Very good agreement is observed in these cases too where the shear stress τ_{xy} has the classic parabolic trend through-the-thickness of the sandwich beam. The maximum shear stress decreases starting from $x = 1.2$ m to $x = 3.6$ m.

4.3 Sandwich circular arch

The final example of this paper examines a circular composite arch. The purpose is to investigate the GDQFEM accuracy for soft-core structures in the presence of curvature. It is worth noticing that, in the previous examples, all the GDQFEM elements were rectangles because the laminae had a rectangular shape. In this case, all the elements must have at least two curved boundaries. So, mapping technique must be used in this case, whereas in the previous examples multi-domain differential quadrature could be directly applied. Both the static and the dynamic analyses of this structure will be discussed. The geometric configuration of the sandwich circular arch is outlined in Fig. 8a), where the two diameters are $D_1 = 6$ m, $D_2 = 8$ m. As far as the mechanical properties are concerned, the top and bottom sheets have $E_f = 30$ MPa, $\nu_f = 0.3$ and density $\rho_f = 2000$ kg/m³ with a thickness $t_f = 0.25$ m. The material of the core is characterized by the value of the elastic modulus $E_c = 30$ kPa, $\nu_c = 0.25$ and density $\rho_c = 100$ kg/m³. The thickness of the core structure is $t_c = 0.5$ m. From Fig. 8a) it appears that the top and bottom layers of the given composite structure are indicated by Ω_f , whereas the core is specified by Ω_c .

In Tab. 5 the first natural frequencies of the sandwich arch are shown for different numbers of grid points. The GDQFEM solutions are compared with the FEM results. Very good agreement is observed. It is also noted that in the some cases a different set of points is used $N \neq M$. In order to have the element compatibility it is sufficient that two adjacent edges have the same number of grid points. For the sake of completeness, the first four mode shapes are graphically depicted in Fig.

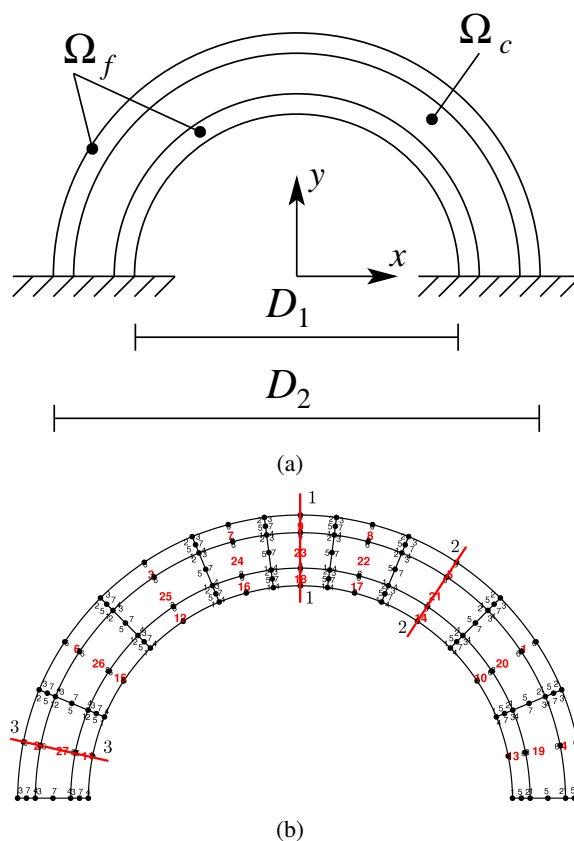


Figure 8: Sandwich circular arch: a) geometric scheme, b) GDQFEM mesh.

9. The soft-core behaviour is very clear from Fig. 9d), because the inner core is squeezed by the stiffer top and bottom layers.

In the second part of this numerical example, the static behavior of the same sandwich arch is studied. The structure is subjected to a uniform pressure $q = 100$ Pa at the external circle radius. The displacement, strain and stress profiles are calculated at three different sections, as indicated in Fig. 8b). The first section 1-1 is the mid-section of the arch. The other two sections are far (section 2-2) and near (section 3-3) the right and left clamped edges, respectively. For the case under study, several stiffness ratios $\chi = E_f/E_c$ are considered. In all the plots of Figs. 10-12 five curves are represented for different values of χ , from $\chi = 10$ (blue curve) to $\chi = 10^5$ (yellow curve). In the plots in hand, the coloured circles are obtained with GDQFEM and the coloured crosses are made by FEM. It is clear that the higher soft-core effect is carried out by the last curve for $\chi = 10^5$. In particular, the Poisson effect of

Table 5: First ten frequencies for a circular composite arch for several grid points.

f [Hz]	FEM‡	$N = 9$	$N = 11$	$N = 15$	$N = 9$	$N = 11$	$N = 13$
		$M = 9$	$M = 11$	$M = 15$	$M = 21$	$M = 21$	$M = 17$
1	0.5524	0.5531	0.5535	0.5531	0.5537	0.5531	0.5529
2	1.1561	1.1588	1.1584	1.1573	1.1580	1.1571	1.1570
3	1.9997	2.0027	2.0023	2.0008	2.0015	2.0004	2.0004
4	2.2463	2.2512	2.2497	2.2483	2.2479	2.2477	2.2479
5	2.6446	2.6459	2.6461	2.6456	2.6458	2.6454	2.6454
6	2.8359	2.8354	2.8354	2.8347	2.8356	2.8346	2.8345
7	3.2546	3.2557	3.2561	3.2554	3.2564	3.2554	3.2551
8	3.8607	3.8602	3.8605	3.8602	3.8612	3.8602	3.8600
9	4.1803	4.1815	4.1805	4.1789	4.1796	4.1786	4.1785
10	4.5884	4.5872	4.5868	4.5869	4.5870	4.5871	4.5870

‡ 2D ABAQUS CPS8R plane elements

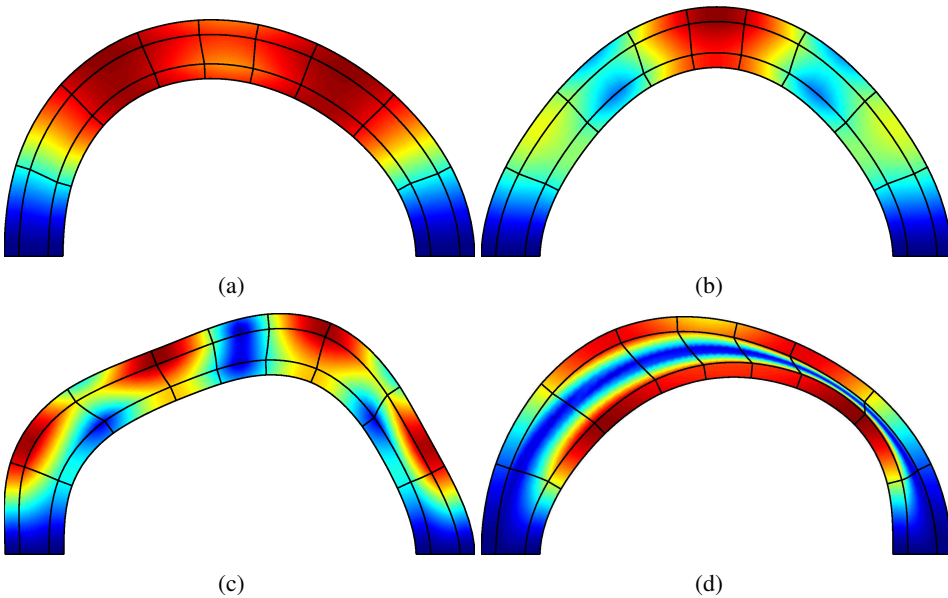


Figure 9: First four mode shapes of a composite circular arch: a) 1st mode, b) 2nd mode, c) 3rd mode, d) 4th mode.

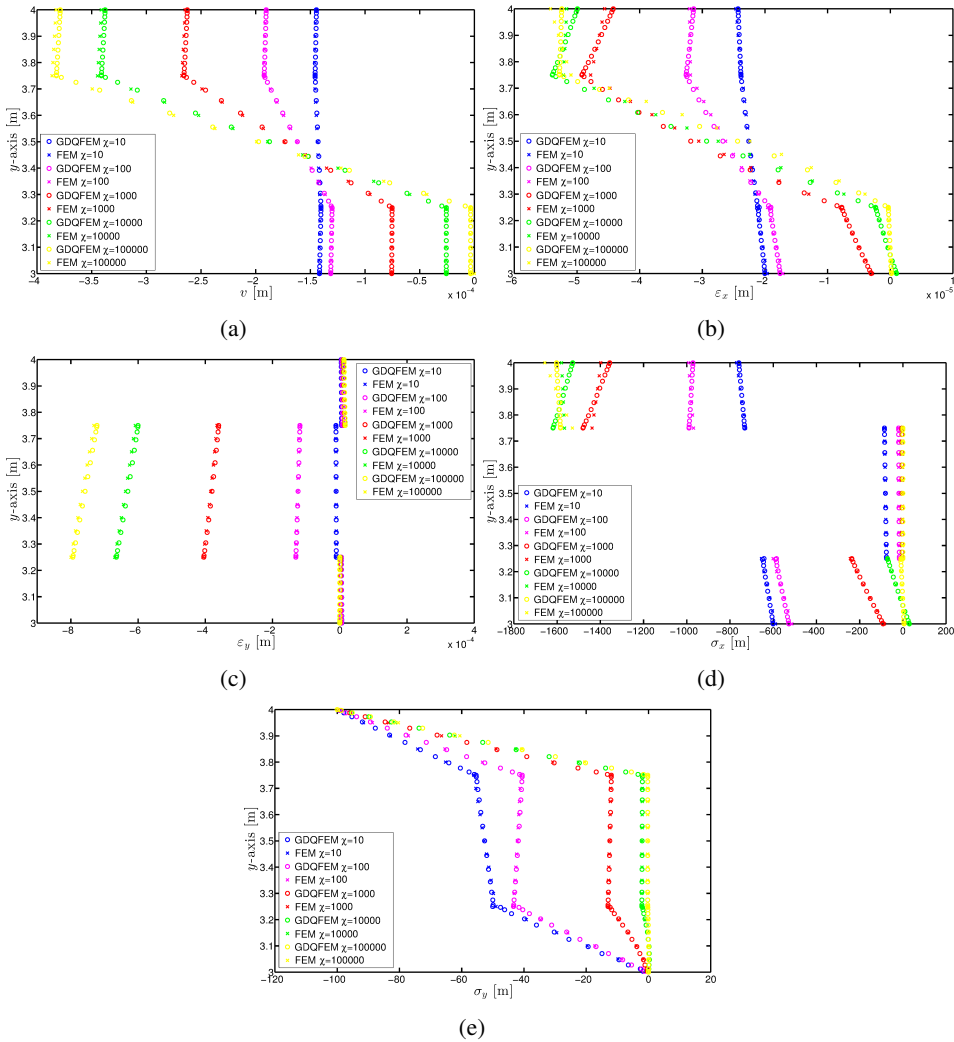


Figure 10: Section 1-1 profiles: a) displacement component v , b) strain component ϵ_x , c) strain component ϵ_y , d) stress component σ_x , e) stress component σ_y .

the core can be seen on the vertical strain component ϵ_y and stress component σ_y . In the first case the deformation of the core is higher than the transversal deformation of the sheets. In the second case, instead, it appears that the normal pressure is concentrated on the top sheets and the energy is fully absorbed by the deformation of the inner soft-core. In Figs. 10a)-e), the profiles of the half section of the arch are represented. In particular, Fig. 10a) shows the vertical displacement, Figs. 10b),c)

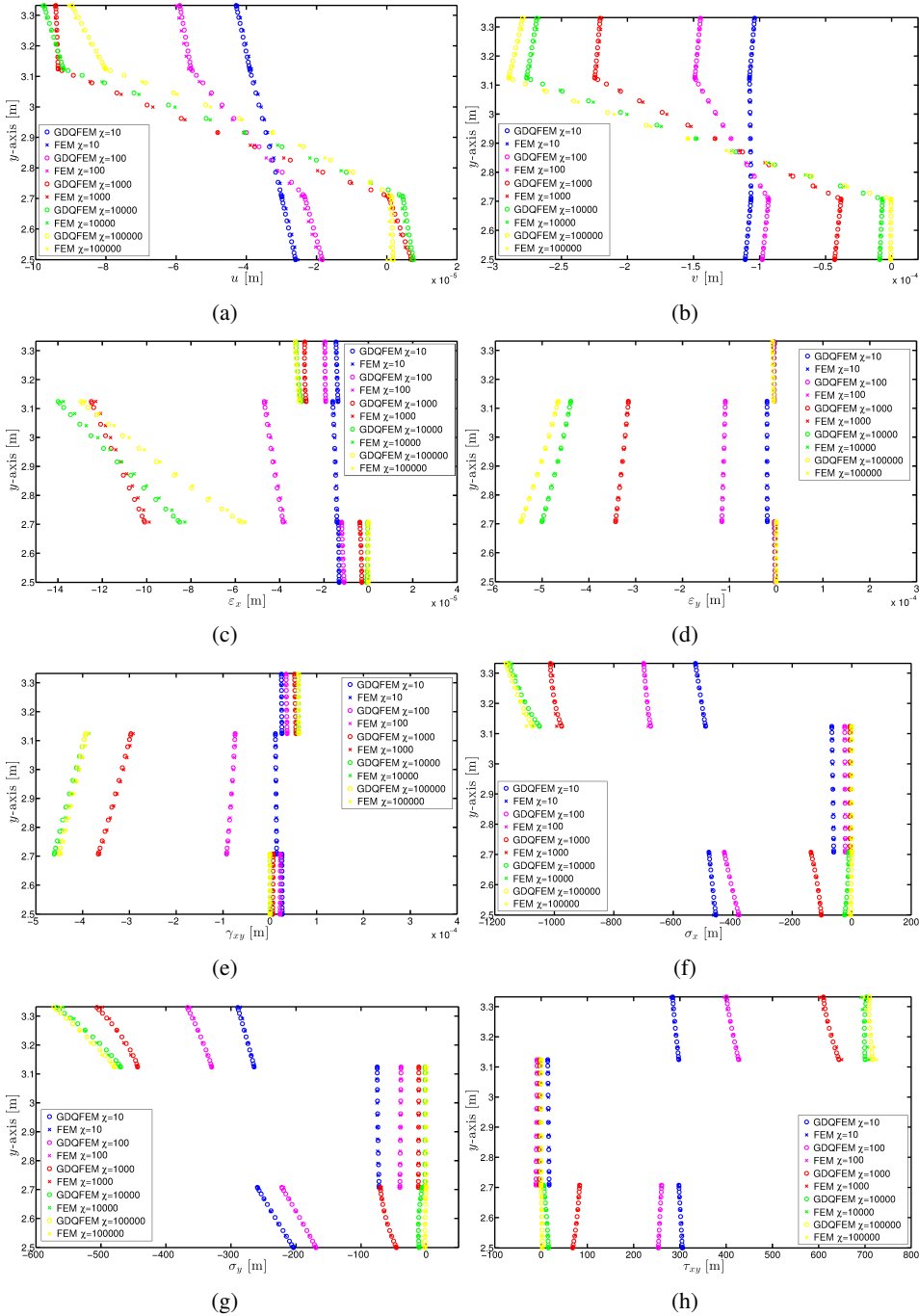


Figure 11: Section 2-2 profiles: a) displacement component u , b) displacement component v , c) strain component ϵ_x , d) strain component ϵ_y , e) strain component γ_{xy} , f) stress component σ_x , g) stress component σ_y , h) stress component τ_{xy} .

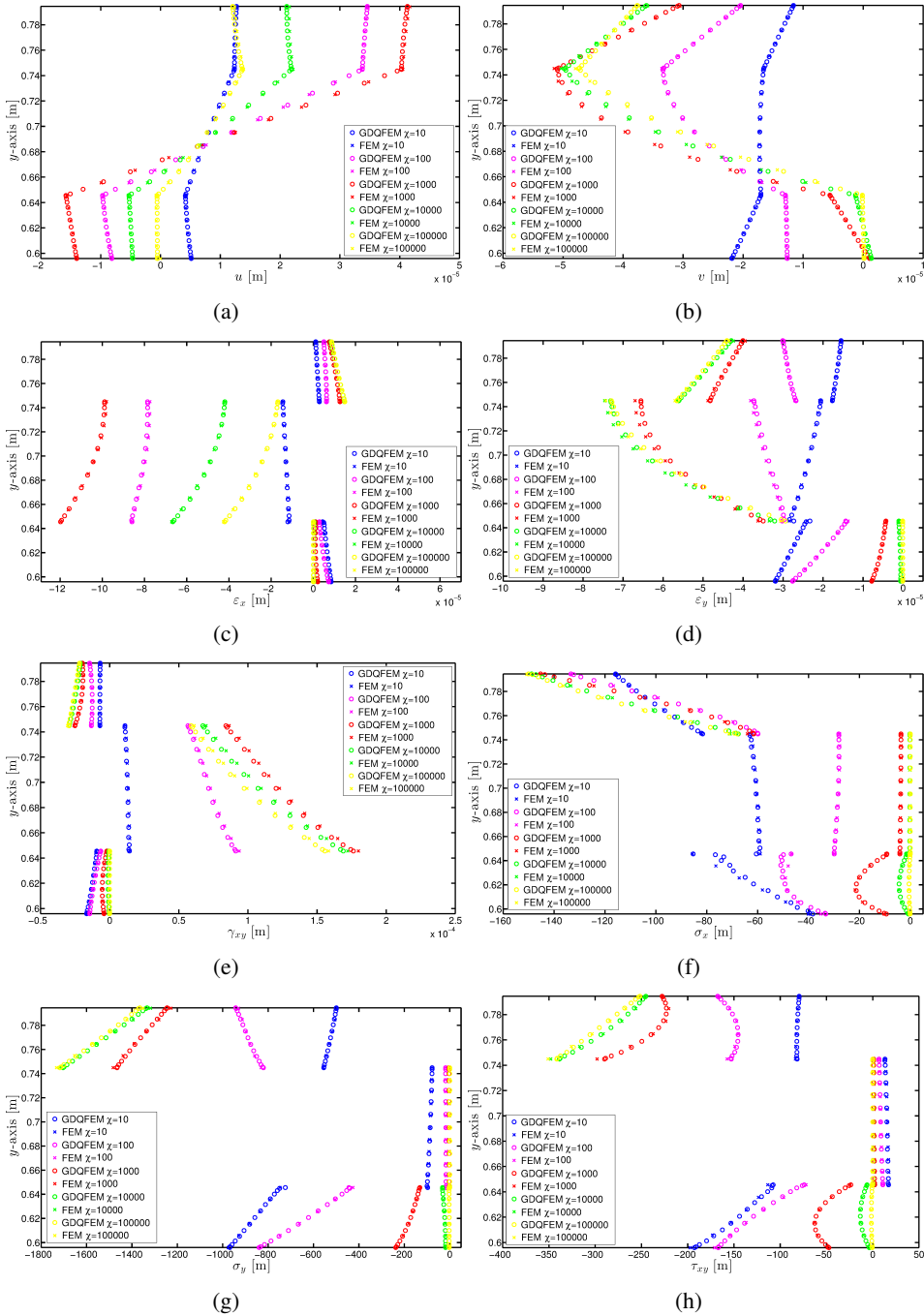


Figure 12: Section 3-3 profiles: a) displacement component u , b) displacement component v , c) strain component ϵ_x , d) strain component ϵ_y , e) strain component γ_{xy} , f) stress component σ_x , g) stress component σ_y , h) stress component τ_{xy} .

show the horizontal and vertical strains components and Figs. 10d),e) show the horizontal and vertical stresses components σ_x and σ_y . Since the arch is symmetric with a symmetric loading, the horizontal displacement u , the shear strain γ_{xy} and the shear stress τ_{xy} are negligible, so they were not depicted. Figs. 11a)-h) show the displacements components u , v , the strain ϵ_x , ϵ_y and γ_{xy} and stress tensor σ_x , σ_y and τ_{xy} in each point of the section 2-2 of Fig. 11b). It is noted that the displacements u and v have a linear trend when $\chi = 10$, whereas the zig-zag effect appears when $\chi \geq 100$. From Figs. 11c)-e) the Poisson effect is clearly concentrated in the core layer only. Finally, from the stress plots described by Figs. 11f)-h), it can be seen that the higher stresses are concentrated on the top layer only due to the soft-core effect of the layer underneath. Finally, in the last section 3-3 the same quantities of section 2-2 are depicted in Figs. 12a)-h). In this last case the soft-core effect is similar to the one of the plots of section 2-2, but the quantities have a non-linear trend through-the-thickness due to the proximity of the external clamped boundary condition. In this case also the GDQFEM numerical solutions are in very good agreement with the reference solution obtained by FEM.

5 Conclusions

In this paper, GDQFEM applications to plane state composite laminated structures have been presented. In particular, both the static and dynamic cases of sandwich beams and arches have been developed comparing the results with FEM and CM. Furthermore, some cases taken from literature have been compared too. It has been observed a very good agreement among all the different numerical methodologies. One the key advantages observed in the computations is the high-accuracy of GDQFEM with respect to commercial codes. In fact, few GDQFEM elements were considered, moreover the degrees of freedom of a GDQFEM model were less than the ones employed in the other techniques. It can be concluded that GDQFEM is a powerful tool for solving laminated composite structures even when the ratios χ between the core and the face sheets are very high. In short, very good accuracy is reached and all the results fits the others obtained with FEM and CM.

Acknowledgement: This research was supported by the Italian Ministry for University and Scientific, Technological Research MIUR (40 % and 60 %). The research topic is one of the subjects of the Centre of Study and Research for the Identification of Materials and Structures (CIMEST)-"M. Capurso" of the University of Bologna (Italy).

References

- Amirani, M. C.; Khalili, S.; Nematì, N.** (2009): Free vibration analysis of sandwich beam with FG core using the element free Galerkin method. *Composite Structures*, vol. 90, no. 3, pp. 373–379.
- Artioli, E.; Gould, P. L.; Viola, E.** (2005): A differential quadrature method solution for shear-deformable shells of revolution. *Engineering Structures*, vol. 27, no. 13, pp. 1879–1892.
- Bert, C. W.; Malik, M.** (1996): The differential quadrature method for irregular domains and application to plate vibration. *International Journal of Mechanical Sciences*, vol. 38, no. 6, pp. 589–606.
- Chen, C.-N.** (1999): The development of irregular elements for differential quadrature element method steady-state heat conduction analysis. *Computer Methods in Applied Mechanics and Engineering*, vol. 170, no. 1-2, pp. 1–14.
- Chen, C.-N.** (1999): The differential quadrature element method irregular element torsion analysis model. *Applied Mathematical Modelling*, vol. 23, no. 4, pp. 309–328.
- Chen, C.-N.** (2000): A generalized differential quadrature element method. *Computer Methods in Applied Mechanics and Engineering*, vol. 188, no. 1-3, pp. 553–566.
- Chen, C.-N.** (2003): DQEM and DQFDM for the analysis of composite two-dimensional elasticity problems. *Composite Structures*, vol. 59, no. 1, pp. 3–13.
- Fantuzzi, N.** (2013): *Generalized Differential Quadrature Finite Element Method applied to Advanced Structural Mechanics*. PhD thesis, University of Bologna, 2013.
- Ferreira, A.; Viola, E.; Tornabene, F.; Fantuzzi, N.; Zenkour, A.** (2013): Analysis of sandwich plates by generalized differential quadrature method. *Mathematical Problems in Engineering*, vol. 2013, pp. 1–12. Article ID 964367, doi:10.1155/2013/964367.
- Ferretti, E.** (2001): *Modellazione del Comportamento del Cilindro Fasciato in Compressione*. PhD thesis, Università del Salento, 2001.
- Ferretti, E.** (2003): Crack propagation modeling by remeshing using the Cell Method (CM). *CMES: Computer Modeling in Engineering & Sciences*, vol. 4, pp. 51–72.
- Ferretti, E.** (2004): A Cell Method (CM) code for modeling the pullout test step-wise. *CMES: Computer Modeling in Engineering & Sciences*, vol. 6, pp. 453–476.

Ferretti, E. (2004): Crack-path analysis for brittle and non-brittle cracks: A Cell Method approach. *CMES: Computer Modeling in Engineering & Sciences*, vol. 6, pp. 227–244.

Ferretti, E. (2004): A discrete nonlocal formulation using local constitutive laws. *International Journal of Fracture*, vol. 130, no. 3, pp. 175–182.

Ferretti, E. (2005): A local strictly nondecreasing material law for modeling softening and size-effect: a discrete approach. *CMES: Computer Modeling in Engineering & Sciences*, vol. 9, pp. 19–48.

Ferretti, E. (2009): Cell Method analysis of crack propagation in tensioned concrete plates. *CMES: Computer Modeling in Engineering & Sciences*, vol. 54, pp. 253–281.

Ferretti, E. (2012): Shape-effect in the effective law of plain and rubberized concrete. *CMC: Computers, Materials, & Continua*, vol. 30, pp. 237–284.

Ferretti, E. (2013): The Cell Method: an enriched description of physics starting from the algebraic formulation. *CMC: Computers, Materials, & Continua*, vol. 36, no. 1, pp. 49–72.

Ferretti, E. (2013): A Cell Method stress analysis in thin floor tiles subjected to temperature variation. *CMC: Computers, Materials, & Continua*, vol. 36, no. 3, pp. 293–322.

Ferretti, E. (2014): *The Cell Method: a purely algebraic computational method in physics and engineering science*. Momentum Press.

Ferretti, E.; Casadio, E.; Leo, A. D. (2008): Masonry walls under shear test: a CM modeling. *CMES: Computer Modeling in Engineering & Sciences*, vol. 30, pp. 163–190.

Han, Z. D.; Liu, H. T.; Rajendran, A. M.; Atluri, S. N. (2006): The applications of Meshless Local Petrov-Galerkin (MLPG) approaches in high-speed impact, penetration and perforation problems. *CMES - Computer Modeling in Engineering and Sciences*, vol. 14, no. 2, pp. 119–128.

Karami, G.; Malekzadeh, P. (2003): Application of a new differential quadrature methodology for free vibration analysis of plates. *International Journal for Numerical Methods in Engineering*, vol. 56, no. 6, pp. 847–868.

Li, Q.; Shen, S.; Han, Z. D.; Atluri, S. N. (2003): Application of Meshless Local Petrov-Galerkin (MLPG) to problems with singularities, and material discontinuities, in 3-d elasticity. *CMES - Computer Modeling in Engineering and Sciences*, vol. 4, no. 5, pp. 571–585.

Li, S.; Atluri, S. N. (2008): The MLPG mixed collocation method for material orientation and topology optimization of anisotropic solids and structures. *CMES - Computer Modeling in Engineering and Sciences*, vol. 30, no. 1, pp. 37–56.

Li, S.; Atluri, S. N. (2008): Topology-optimization of structures based on the MLPG mixed collocation method. *CMES - Computer Modeling in Engineering and Sciences*, vol. 26, no. 1, pp. 61–74.

Liu, F.-L. (1999): Differential quadrature element method for static analysis of shear deformable cross-ply laminates. *International Journal for Numerical Methods in Engineering*, vol. 46, no. 8, pp. 1203–1219.

Marzani, A.; Tornabene, F.; Viola, E. (2008): Nonconservative stability problems via generalized differential quadrature method. *Journal of Sound & Vibration*, vol. 315, no. 1-2, pp. 176–196.

Shu, C. (2000): *Differential Quadrature and Its Applications in Engineering*. Springer Verlag.

Shu, C.; Chen, W.; Du, H. (2000): Free vibration analysis of curvilinear quadrilateral plates by the differential quadrature method. *Journal of Computational Physics*, vol. 163, no. 2, pp. 452–466.

Sladek, J.; Sladek, V.; Atluri, S. N. (2004): Meshless Local Petrov-Galerkin method for heat conduction problem in an anisotropic medium. *CMES - Computer Modeling in Engineering and Sciences*, vol. 6, no. 3, pp. 309–318.

Tonti, E. (2001): A direct discrete formulation of field laws: the Cell Method. *CMES: Computer Modeling in Engineering & Sciences*, vol. 2, pp. 237–258.

Tornabene, F. (2009): Free vibration analysis of functionally graded conical, cylindrical and annular shell structures with a four-parameter power-law distribution. *Computer Methods in Applied Mechanics and Engineering*, vol. 198, no. 37-40, pp. 2911–2935.

Tornabene, F. (2011): 2-D GDQ solution for free vibrations of anisotropic doubly-curved shells and panels of revolution. *Composite Structures*, vol. 93, pp. 1854–1876.

Tornabene, F. (2011): Free vibration of laminated composite doubly-curved shells and panels of revolution via GDQ method. *Computer Methods in Applied Mechanics and Engineering*, vol. 200, pp. 931–952.

Tornabene, F. (2011): Free vibrations of anisotropic doubly-curved shells and panels of revolution with a free-form meridian resting on Winkler-Pasternak elastic foundations. *Composite Structures*, vol. 94, pp. 186–206.

Tornabene, F. (2012): *Meccanica delle Strutture a Guscio in Materiale Composito. Il Metodo Generalizzato di Quadratura Differenziale*. Esculapio.

Tornabene, F.; Ceruti, A. (2013): Free-form laminated doubly-curved shells and panels of revolution on Winkler-Pasternak elastic foundations: A 2D GDQ solution for static and free vibration analysis. *World Journal of Mechanics*, vol. 3, pp. 1–25.

Tornabene, F.; Ceruti, A. (2013): Mixed static and dynamic optimization of four-parameter functionally graded completely doubly-curved and degenerate shells and panels using GDQ method. *Mathematical Problems in Engineering*, vol. 2013, pp. 1–33.

Tornabene, F.; Fantuzzi, N.; Viola, E.; Carrera, E. (2014): Static analysis of doubly-curved anisotropic shells and panels using CUF approach, differential geometry and differential quadrature method. *Composite Structures*, vol. 107, pp. 675–697.

Tornabene, F.; Fantuzzi, N.; Viola, E.; Cinefra, M.; Carrera, E.; Ferreira, A.; Zenkour, A. (2014): Analysis of thick isotropic and cross-ply laminated plates by generalized differential quadrature method and a unified formulation. *Composite Part B Engineering*. In Press.

Tornabene, F.; Fantuzzi, N.; Viola, E.; Ferreira, A. J. M. (2013): Radial basis function method applied to doubly-curved laminated composite shells and panels with a general higher-order equivalent single layer theory. *Composite Part B Engineering*, vol. 55, pp. 642–659.

Tornabene, F.; Fantuzzi, N.; Viola, E.; Reddy, J. N. (2013): Winkler-Pasternak foundation effect on the static and dynamic analyses of laminated doubly-curved and degenerate shells and panels. *Composite Part B Engineering*. In Press.

Tornabene, F.; Liverani, A.; Caligiana, G. (2011): FGM and laminated doubly-curved shells and panels of revolution with a free-form meridian: a 2-D GDQ solution for free vibrations. *International Journal of Mechanical Sciences*, vol. 53, pp. 446–470.

Tornabene, F.; Liverani, A.; Caligiana, G. (2012): General anisotropic doubly-curved shell theory: a differential quadrature solution for free vibrations of shells and panels of revolution with a free-form meridian. *Journal of Sound & Vibration*, vol. 331, pp. 4848–4869.

Tornabene, F.; Liverani, A.; Caligiana, G. (2012): Laminated composite rectangular and annular plates: A GDQ solution for static analysis with a posteriori shear and normal stress recovery. *Composite Part B Engineering*, vol. 43, pp. 1847–1872.

Tornabene, F.; Liverani, A.; Caligiana, G. (2012): Static analysis of laminated composite curved shells and panels of revolution with a posteriori shear and normal stress recovery using generalized differential quadrature method. *International Journal of Mechanical Sciences*, vol. 61, pp. 71–87.

Tornabene, F.; Marzani, A.; Viola, E.; Elishakoff, I. (2010): Critical flow speeds of pipes conveying fluid by the generalized differential quadrature method. *Advances in Theoretical and Applied Mechanics*, vol. 3, no. 3, pp. 121–138.

Tornabene, F.; Reddy, J. (2014): FGM and laminated doubly-curved and degenerate shells resting on nonlinear elastic foundation: a GDQ solution for static analysis with a posteriori stress and strain recovery. *Journal of Indian Institute of Science*, vol. 57, pp. 269–296.

Tornabene, F.; Viola, E. (2007): Vibration analysis of spherical structural elements using the GDQ method. *Computers & Mathematics with Applications*, vol. 53, no. 10, pp. 1538–1560.

Tornabene, F.; Viola, E. (2008): 2-D solution for free vibrations of parabolic shells using generalized differential quadrature method. *European Journal of Mechanics - A/Solids*, vol. 27, no. 6, pp. 1001–1025.

Tornabene, F.; Viola, E. (2009): Free vibration analysis of functionally graded panels and shells of revolution. *Meccanica*, vol. 44, no. 3, pp. 255–281.

Tornabene, F.; Viola, E. (2009): Free vibrations of four-parameter functionally graded parabolic panels and shell of revolution. *European Journal of Mechanics - A/Solids*, vol. 28, no. 5, pp. 991–1013.

Tornabene, F.; Viola, E. (2013): Static analysis of functionally graded doubly-curved shells and panels of revolution. *Meccanica*, vol. 48, pp. 901–930.

Tornabene, F.; Viola, E.; Fantuzzi, N. (2013): General higher-order equivalent single layer theory for free vibrations of doubly-curved laminated composite shells and panels. *Composite Structures*, vol. 104, pp. 94–117.

Tornabene, F.; Viola, E.; Inman, D. J. (2009): 2-D differential quadrature solution for vibration analysis of functionally graded conical, cylindrical and annular shell structures. *Journal of Sound & Vibration*, vol. 328, no. 3, pp. 259–290.

Viola, E.; Dilena, M.; Tornabene, F. (2007): Analytical and numerical results for vibration analysis of multi-stepped and multi-damaged circular arches. *Journal of Sound & Vibration*, vol. 299, no. 1-2, pp. 143–163.

Viola, E.; Rossetti, L.; Fantuzzi, N. (2012): Numerical investigation of functionally graded cylindrical shells and panels using the generalized unconstrained third order theory coupled with the stress recovery. *Composite Structures*, vol. 94, pp. 3736–3758.

- Viola, E.; Tornabene, F.** (2005): Vibration analysis of damaged circular arches with varying cross-section. *Structural Integrity & Durability (SID-SDHM)*, vol. 1, no. 2, pp. 155–169.
- Viola, E.; Tornabene, F.** (2006): Vibration analysis of conical shell structures using GDQ method. *Far East Journal of Applied Mathematics*, vol. 25, no. 1, pp. 23–39.
- Viola, E.; Tornabene, F.** (2009): Free vibrations of three parameter functionally graded parabolic panels of revolution. *Mechanics Research Communications*, vol. 36, no. 5, pp. 587–594.
- Viola, E.; Tornabene, F.; Fantuzzi, N.** (2013): General higher-order shear deformation theories for the free vibration analysis of completely doubly-curved laminated shells and panels. *Composite Structures*, vol. 95, pp. 639–666.
- Viola, E.; Tornabene, F.; Fantuzzi, N.** (2013): Generalized differential quadrature finite element method for cracked composite structures of arbitrary shape. *Composite Structures*, vol. 106, pp. 815–834.
- Viola, E.; Tornabene, F.; Fantuzzi, N.** (2013): Static analysis of completely doubly-curved laminated shells and panels using general higher-order shear deformation theories. *Composite Structures*, vol. 101, pp. 59–93.
- Xing, Y.; Liu, B.** (2009): High-accuracy differential quadrature finite element method and its application to free vibrations of thin plate with curvilinear domain. *International Journal for Numerical Methods in Engineering*, vol. 80, no. 13, pp. 1718–1742.
- Xing, Y.; Liu, B.; Liu, G.** (2010): A differential quadrature finite element method. *International Journal of Applied Mechanics*, vol. 2, pp. 207–227.
- Zhong, H.; He, Y.** (1998): Solution of Poisson and Laplace equations by quadrilateral quadrature element. *International Journal of Solids and Structures*, vol. 35, no. 21, pp. 2805–2819.
- Zhong, H.; Yu, T.** (2009): A weak form quadrature element method for plane elasticity problems. *Applied Mathematical Modelling*, vol. 33, no. 10, pp. 3801–3814.
- Zong, Z.; Zhang, Y.** (2009): *Advanced Differential Quadrature Methods*. Chapman & Hall/CRC Applied Mathematics & Nonlinear Science. Taylor & Francis.

